

A Two-Level Machine Learning Framework for Managing EV Charging and Renewable Energy Curtailment in Smart Grids

Fatemeh Nasr Esfahani

School of Engineering

Lancaster University

Lancaster, UK

f.nasresfahani@lancaster.ac.uk

Neeraj Suri

School of Computing and Communications

Lancaster University

Lancaster, UK

neeraj.suri@lancaster.ac.uk

Xiandong Ma

School of Engineering

Lancaster University

Lancaster, UK

xiandong.ma@lancaster.ac.uk

Abstract—The increasing integration of electric vehicles (EVs) and renewable energy sources (RES) into power grids introduces significant challenges in managing dynamic energy demands and ensuring grid stability. This paper proposes a comprehensive two-level machine learning (ML) and optimisation framework for intelligent energy management in EV- and RES-integrated smart grids. In the prediction layer, supervised ML models, including Random Forest (RF) and Gradient Boosting (GB), accurately forecast EV charging demand and renewable generation. These forecasts are then fed into the optimisation layer, where a multi-objective particle swarm optimisation (PSO) algorithm minimises power losses, optimises EV charging schedules, and reduces renewable curtailment while ensuring voltage stability. The framework is evaluated on a modified IEEE 14-bus system incorporating EV charging stations, photovoltaics (PV), and wind turbines. Simulation results validate the effectiveness of the proposed framework, demonstrating a reduction in renewable energy curtailment and improved computational efficiency compared to benchmark optimisation methods.

Index Terms—Electric Vehicles, Smart Grids, Renewable Energy Integration, Machine Learning.

I. INTRODUCTION

As modern power systems evolve to meet the increasing demand for cleaner and more efficient energy solutions, electric vehicles (EVs) and renewable energy sources (RESs) play an essential role in decarbonising both the electricity and transportation sectors [1]–[3]. However, the large-scale integration of EVs and RESs introduces complex technical challenges for modern power grids [4]–[6]. In particular, the rapid adoption of EVs is revolutionising the transportation sector while simultaneously reshaping power systems by introducing dynamic, decentralised, and unpredictable energy demands [4]. Unlike traditional loads, EV charging behaviour is driven by consumer preferences and travel habits, resulting in demand spikes that are difficult to predict and manage. High penetration of RESs further compounds these challenges due to their variable and intermittent generation [5], [6].

The simultaneous variability of the demand for EV charging and the generation of RES disrupts the stability of the grid, causing voltage fluctuations and frequency deviations [4], [6], [7]. Traditional centralised energy management systems are of-

ten inadequate for managing these dynamics, prompting a shift towards distributed, intelligent energy management strategies aimed at improving reliability and operational efficiency [8].

Various distributed optimisation frameworks have been developed to enhance grid stability under high RES and EV penetration. For example, a joint distributed optimisation approach in [4] addresses voltage control and coordinated scheduling of energy storage and EV charging, but it lacks predictive capabilities for proactive management. More advanced strategies, including hierarchical control methods in [9], [10] and two-stage optimisations combining particle swarm optimisation (PSO) and mixed-integer linear programming (MILP) in [7], offer improvements in scalability, resilience, and computational efficiency. However, even these approaches largely rely on fixed control structures, limiting adaptability to dynamic, real-time grid conditions.

To address the limitations of fixed and reactive control strategies, machine learning (ML) techniques have been increasingly adopted to enable proactive and dynamic energy management by forecasting key grid parameters, such as RES generation and EV demand [11]. Studies employing ML models, such as random forest (RF), convolutional neural networks (CNN), recurrent neural networks (RNN), gradient boosting (GB), and long short-term memory (LSTM) demonstrate ML’s potential in forecasting and optimisation for smart grids [12]. In addition, heuristic optimisation methods such as genetic algorithms (GA) have been applied for solving related scheduling and control problems [13], [14]. Comprehensive reviews, such as [15] and [16], highlight significant advances in ML-based forecasting. They also identify a gap in the integration of these predictive models with real-time multi-objective optimisation frameworks for operational decision-making. Some studies have begun to bridge this gap by combining forecasting with optimisation. For instance, [17] presents an LSTM-based demand prediction model coupled with optimised EV charging strategies. While valuable, this study focuses primarily on intelligent pricing and discharge scheduling, rather than addressing broader multi-objective optimisation goals, such as power loss minimisation, renewable

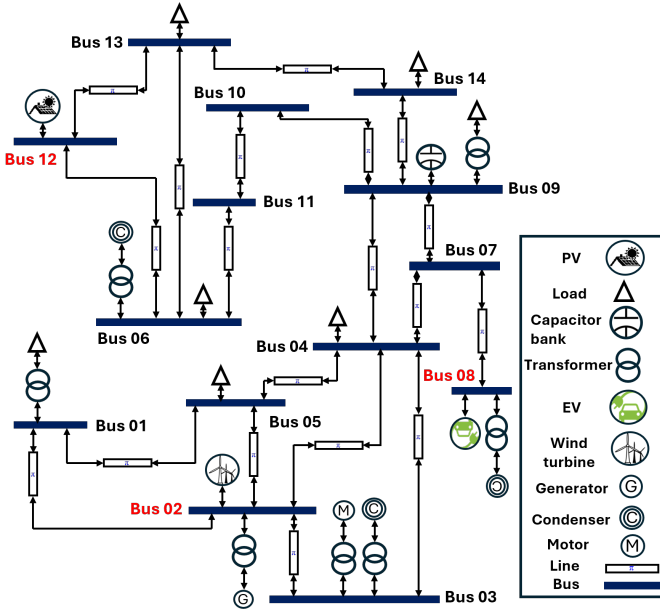


Fig. 1: Schematic representation of the IEEE 14-bus power grid system with key components.

curtailment reduction, and voltage stability enhancement.

Building on these insights, although significant progress has been made in both distributed optimisation and ML-based forecasting, a clear gap remains: the lack of comprehensive frameworks that integrate accurate predictions with real-time, multi-objective optimisation strategies for EV- and RES-integrated smart grids. To bridge this gap, a two-level ML and optimisation framework is proposed in this paper. The first layer, namely the prediction layer, employs ensemble learning models, including RF and GB, to forecast key grid parameters, such as EV charging demand and renewable energy generation. Compared to deep learning models like LSTM, the models used in this paper (i.e., RF and GB) offer a favourable balance between accuracy and computational efficiency, making them particularly suitable for real-time applications with limited data. These models also naturally handle heterogeneous inputs, including temporal (hour of day, day type) and weather-related features (temperature, solar irradiance, wind speed). The second layer, namely the optimisation layer, incorporates the forecasts into a multi-objective PSO algorithm. This optimisation simultaneously minimises power losses and schedules EV charging, thereby enhancing grid stability and operational efficiency. The optimisation also respects key operational constraints, including voltage limits, power balance, EV charging capacities, and renewable generation thresholds, ensuring feasibility and safe grid operation. The paper utilises the IEEE 14-bus system shown in Fig. 1 as a benchmark, which consists of 14 buses, 19 branches, and various components, such as generators and different loads. For the purposes of this study, the IEEE 14-bus system is modified to include EV charging infrastructure and RESs (e.g., wind turbines and photovoltaics (PV)).

The rest of this paper is organised as follows: Section II formulates the problem and outlines the mathematical framework for optimisation. Section III discusses the proposed methodology, including the developed ML models and the optimisation algorithm. Section IV presents performance evaluations. Finally, Section V concludes the paper.

II. PROBLEM FORMULATION: COST FUNCTION AND CONSTRAINTS

A two-level optimisation framework is developed in this paper, combining ML-based forecasting and system-wide optimisation. The framework focuses on minimising global objectives, such as power losses and renewable energy curtailment, while efficiently managing EV charging and discharging across the grid. A comprehensive cost function is formulated to balance energy efficiency and EV charging satisfaction, and a set of operational constraints, including power flow equations, voltage limits, EV scheduling bounds, and renewable energy limits, is incorporated to ensure safe and reliable grid operation.

A. Cost function

The cost function reflects the dual objectives of minimising power losses and efficiently managing EV charging. The total cost is defined as:

$$\mathcal{J}_{\text{total}} = \alpha_1 \mathcal{J}_{\text{loss}} + \alpha_2 \mathcal{J}_{\text{EV}}, \quad (1)$$

where $\mathcal{J}_{\text{loss}}$ represents the power losses in the grid caused by resistive elements. Minimising $\mathcal{J}_{\text{loss}}$ reduces energy wastage and improves grid efficiency. \mathcal{J}_{EV} captures penalties for unmet EV charging demands, ensuring user needs are met while avoiding overloading the grid. α_1, α_2 are adjustable weights to balance the importance of power losses and EV charging efficiency.

1) *Power Loss Costs ($\mathcal{J}_{\text{loss}}$):* Power losses are modelled as:

$$\mathcal{J}_{\text{loss}} = c_{\text{loss}} \cdot \sum_{t=1}^T \sum_{(i,j) \in \mathcal{L}} \frac{P_{ij,t}^2 + Q_{ij,t}^2}{V_i^2}, \quad (2)$$

where $P_{ij,t}$ and $Q_{ij,t}$ represent the active and reactive power flows on branch (i, j) at time t . Also, V_i denotes the voltage magnitude at node i , c_{loss} is the cost coefficient associated with power losses, \mathcal{L} represents the set of all branches (or transmission lines) in the power network, and T is the total number of time steps (or time periods) in the analysis.

2) *EV Costs (\mathcal{J}_{EV}):* This term captures penalties for unmet EV charging demands:

$$\mathcal{J}_{\text{EV}} = \sum_{t=1}^T (c_{\text{penalty}} \cdot P_{\text{Unmet},t}), \quad (3)$$

where $P_{\text{Unmet},t}$ represents the total unmet EV charging demand at time t , and c_{penalty} is the penalty coefficient applied for unmet charging demand.

B. Constraints

The optimisation problem is subject to the constraints listed in Table I, which ensure the safe and efficient operation of the grid. Power flow constraints enforce Kirchhoff's laws for active and reactive power to maintain the balance of power flows within the grid. Here, $P_{load,i,t}$ and $Q_{load,i,t}$ represent the active and reactive power demands at node i at time t . Voltage limits ensure that voltage magnitudes at each node remain within the permissible range $[V_{min}, V_{max}]$, where V_{min} and V_{max} denote the minimum and maximum allowable voltages, respectively. EV scheduling constraints aggregate the total charging and discharging power contributions of all EVs in the system, ensuring that the total power does not exceed $P_{EV,max}$. Similarly, the renewable energy constraints ensure that the total renewable energy generated R_{gen} at any time t does not exceed the installed capacity R_{cap} , and renewable curtailment $R_{curt,t}$ ensures that excess renewable energy can be managed to maintain grid stability. In these expressions, \mathcal{N} represents the set of nodes in the grid and \mathcal{EV} represents the set of all EVs in the system.

TABLE I: Constraints of the optimisation problem

Constraint Type	Mathematical Expression
Power Flow	$P_i - \sum_{(i,j) \in \mathcal{L}} P_{ij,t} = P_{load,i,t}$
	$Q_i - \sum_{(i,j) \in \mathcal{L}} Q_{ij,t} = Q_{load,i,t}$
Voltage Limits	$V_{min} \leq V_i \leq V_{max}, \quad \forall i \in \mathcal{N}$
EV Scheduling	$0 \leq \sum_{i \in \mathcal{EV}} P_{EV,i,t} \leq P_{EV,max}$
Renewable Energy	$R_{gen,t} \leq R_{cap}$
Curtailment	$0 \leq R_{curt,t} \leq R_{gen,t}$

III. PROPOSED TWO-LEVEL ML FRAMEWORK

To address the challenges of real-time energy management in EV-integrated smart grids, a two-level ML framework is proposed. This framework integrates prediction and optimisation to dynamically manage grid operations while minimising costs, as shown in Fig. 2.

A. Prediction layer

The first layer of the framework employs supervised ML models to predict key grid parameters. These predictions provide the optimisation layer with real-time data to enable informed decision-making while considering dynamic grid conditions.

1) *EV Demand Prediction*: Accurate prediction of EV charging demand ($P_{EV,i,t}$) is a critical component of the framework, enabling real-time optimisation of grid operations. A supervised ML approach using the RF algorithm is used here to forecast demand based on historical data and contextual features. This algorithm is outlined in Algorithm 1 and consists of the following steps:

Firstly, the ‘‘data pre-processing’’ step prepares the input data for training and prediction. Missing values in any feature F are interpolated using linear interpolation:

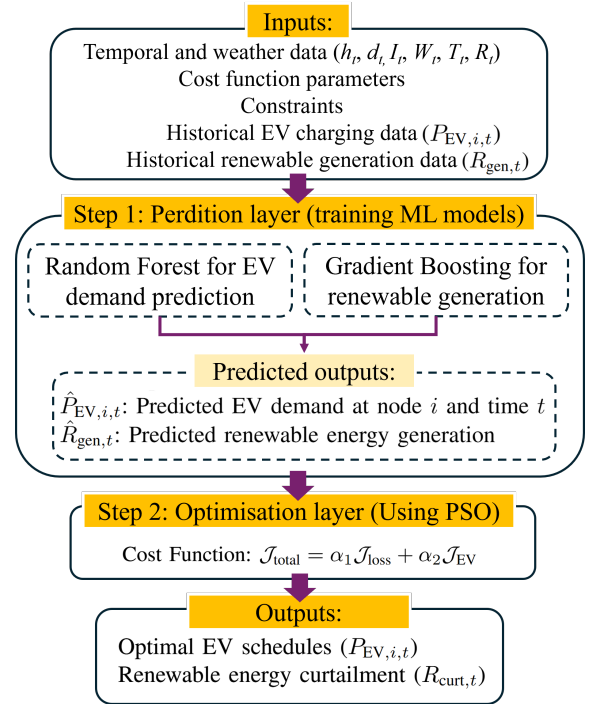


Fig. 2: Flowchart of the proposed two-level ML framework for EV- and RES-integrated smart grid optimisation.

$$F_{interpolated} = F_{previous} + \frac{F_{next} - F_{previous}}{t_{next} - t_{previous}} \times (t - t_{previous}). \quad (4)$$

Next, all features are normalised using Min-Max scaling $F_{scaled} = \frac{F - F_{min}}{F_{max} - F_{min}}$, ensuring a uniform range of $[0, 1]$, which enhances model performance.

Next, in the ‘‘feature engineering’’ step, raw data is transformed into meaningful input vectors for the ML model. Temporal features such as hour of the day (h_t) and day type (d_t), distinguishing between weekdays and weekends, are extracted for each timestamp t . Additionally, weather data, including temperature (T_t), rainfall (R_t), and humidity (H_t), are combined with these temporal features to form input vectors: $X_{t_1} = \{h_t, d_t, T_t, R_t, H_t\}$.

Then, the ‘‘RF model training’’ step takes place, which consists of multiple decision trees for EV demand prediction. For each tree T_n in the forest, a bootstrap sample of the dataset is created by randomly sampling data points with replacement. Each tree is trained on its bootstrapped dataset, and the final prediction is obtained by aggregating outputs from all trees. For a given input X_{t_1} , the predicted EV demand $\hat{P}_{EV,i,t}$ is calculated as:

$$\hat{P}_{EV,i,t} = \frac{1}{N_{trees}} \sum_{n=1}^{N_{trees}} T_n(X_{t_1}). \quad (5)$$

After that, once the model is trained, it is used in the ‘‘prediction’’ step to estimate EV demand for new input data

in the test set. For each input vector X_{t_1} , the predicted EV demand for each node i in the grid at each time step t is computed using the same aggregation technique across all decision trees.

Finally, in the “validation” step, the performance of the trained model is evaluated using mean absolute percentage error (MAPE) over the total number of predictions (i.e., $\mathcal{N} \times T$).

Algorithm 1 RF for EV demand prediction

- 1: **Input:**
 Historical EV charging data ($P_{EV,i,t}$) for nodes $i = 1, 2, \dots, \mathcal{N}$ and time steps $t = 1, 2, \dots, T$;
 Weather data (T_t, R_t, H_t);
 Temporal data (h_t, d_t).
- 2: **Step 1: Data pre-processing**
- 3: **for** each feature F in the dataset **do**
- 4: **if** F contains missing values **then**
- 5: Interpolate missing values for F
- 6: **end if**
- 7: **end for**
- 8: Normalise features F_{scaled} using Min-Max scaling.
- 9: **Step 2: Feature engineering**
- 10: **for** each timestamp t **do**
- 11: Extract temporal features (h_t, d_t)
- 12: Combine (T_t, R_t, H_t) and (h_t, d_t) into X_{t_1}
- 13: **end for**
- 14: **Step 3: Train RF model**
- 15: **for** each tree n in the Random Forest ($n = 1, 2, \dots, N_{\text{trees}}$) **do**
- 16: Train decision tree T_n using bootstrapped samples of $X_{t_1}, P_{EV,i,t}$
- 17: **end for**
- 18: Aggregate predictions across all trees: $\hat{P}_{EV,i,t}$
- 19: **Step 4: Prediction**
- 20: **for** each data point in the test set **do**
- 21: Predict $\hat{P}_{EV,i,t}$ using the trained RF model.
- 22: **end for**
- 23: **Step 5: Validation**
- 24: Compute performance metrics:

$$\text{MAPE} = \frac{1}{\mathcal{N} \times T} \sum_{i=1}^{\mathcal{N} \times T} \left| \frac{P_{EV,i,t} - \hat{P}_{EV,i,t}}{P_{EV,i,t}} \right| \times 100$$

2) *Renewable generation prediction:* Accurately forecasting renewable energy generation ($R_{\text{gen},t}$) is essential for managing grid stability and ensuring the efficient utilisation of renewable resources. A GB algorithm is employed to predict renewable generation using weather features such as solar irradiance, wind speed, and temperature. The algorithm is outlined in Algorithm 2 and is described below:

Firstly, in the “data pre-processing” step, weather features representing solar irradiance (I_t), wind speed (W_t), and temperature (T_t) are normalised using Min-Max scaling to ensure uniform feature ranges. Similar to the EV demand prediction

algorithm, missing values in the weather dataset are handled using linear interpolation.

Next, in the “feature engineering” step, temporal features (h_t, d_t) representing the hour of the day and day type (week-day/weekend) are combined with weather data, including solar irradiance (I_t), wind speed W_t , and temperature (T_t) to form input vectors: $X_{t_2} = \{h_t, d_t, I_t, W_t, T_t\}$.

Then, the “GB algorithm” constructs an ensemble of decision trees to iteratively minimise a loss function, such as mean squared error (MSE):

$$\text{MSE} = \frac{1}{\mathcal{N} \times T} \sum_{t=1}^{\mathcal{N} \times T} \left(R_{\text{gen},t} - \hat{R}_{\text{gen},t} \right)^2 \quad (6)$$

After that, in the “prediction” step, for each input vector X_{t_2} in the test dataset, the trained GB model predicts renewable generation ($\hat{R}_{\text{gen},t}$). The final predicted renewable generation is obtained by aggregating predictions from all trees:

$$\hat{R}_{\text{gen},t} = \sum_{m=1}^M \alpha_m T_m(X_{t_2}), \quad (7)$$

where α_m is the learning rate, T_m is the m^{th} tree, and M is the total number of trees.

Finally, the model’s performance is evaluated using the root mean squared error (RMSE).

B. Optimisation layer using PSO

The optimisation layer employs the predicted values from the ML models to solve a multi-objective problem. As outlined in Section II, the primary objectives are to minimise power losses in the grid ($\mathcal{J}_{\text{loss}}$) and to optimise EV charging schedules (\mathcal{J}_{EV}) to reduce unmet EV demand while ensuring grid stability by satisfying the constraints listed in Table I.

The optimisation problem is solved using PSO, which is effective for handling complex, nonlinear, and multi-dimensional problems. PSO operates based on a population of particles, each representing a candidate solution, and iteratively improves these solutions based on the objective function. Optimisation using PSO is presented in Algorithm 3 and is carried out as follows:

Firstly, a population of particles is created, where each particle represents a potential solution comprising EV schedules ($P_{EV,i,t}$) and renewable energy curtailment decisions ($R_{\text{curt},t}$). Each particle is assigned a random initial velocity to facilitate exploration of the solution space. Additionally, bounds for the decision variables are defined to ensure feasible solutions. Next, each particle’s fitness is evaluated using the cost function $\mathcal{J}_{\text{total}}$ in (1). Then, each particle’s solution is evaluated against the constraints outlined in Table I. After that, each particle’s velocity and position are updated based on their own best-known position and the global best-known position of the swarm:

$$\begin{cases} v_{i,k+1} = \omega v_{i,k} + c_1 r_1 (p_{\text{best}} - x_{i,k}) + c_2 r_2 (g_{\text{best}} - x_{i,k}) \\ x_{i,k+1} = x_{i,k} + v_{i,k+1} \end{cases}, \quad (8)$$

Algorithm 2 GB Algorithm for renewable generation prediction

- 1: **Input:**
Weather data (I_t, W_t, T_t) ;
Temporal data (h_t, d_t) ;
Historical renewable generation data $(R_{\text{gen},t})$.
- 2: **Step 1: Data pre-processing**
- 3: **for** each feature F in the dataset **do**
- 4: **if** F contains missing values **then**
- 5: Interpolate missing values for F
- 6: **end if**
- 7: **end for**
- 8: Normalise features F_{scaled} using Min-Max scaling.
- 9: **Step 2: Feature engineering**
- 10: **for** each timestamp t **do**
- 11: Extract temporal features (h_t, d_t)
- 12: Combine (I_t, W_t, T_t) and (h_t, d_t) into X_{t_2}
- 13: **end for**
- 14: **Step 3: Train GB model**
- 15: **for** each tree m in the GB model ($m = 1, 2, \dots, M$) **do**
- 16: Train decision tree T_m to minimise MSE
- 17: **end for**
- 18: Aggregate predictions across all trees.
- 19: **Step 4: Prediction**
- 20: **for** each data point X_t in the test set **do**
- 21: Predict renewable generation $\hat{R}_{\text{gen},t}$ using the trained GB model
- 22: **end for**
- 23: **Step 5: Validation**
- 24: Compute $\text{RMSE} = \sqrt{\frac{1}{\mathcal{N} \times T} \sum_{t=1}^{\mathcal{N} \times T} (R_{\text{gen},t} - \hat{R}_{\text{gen},t})^2}$

where ω is the inertia weight, c_1, c_2 are acceleration coefficients, r_1, r_2 are random numbers, p_{best} is the particle's best position, and g_{best} is the swarm's global best position.

Finally, the algorithm terminates when the maximum number of iterations is reached or the change in fitness value across iterations falls below a predefined threshold.

IV. CASE STUDY AND RESULTS

This section presents the simulation results of the proposed framework for energy management in smart grids integrated with EVs and RESs. The framework is evaluated on the modified IEEE 14-bus test system shown in Fig. 1.

A. Prediction layer performance

The prediction layer uses the two supervised ML algorithms to forecast the demand for EV charging and the generation of renewable energy. The models are trained on historical datasets that reflect daily variability.

1) *EV charging demand prediction*: Following the methodology described in Subsection III-A1, the RF model is employed to forecast hourly EV charging demand at Bus 08. The model uses a set of carefully engineered features, including temporal features (hour of day, day type) and contextual

Algorithm 3 PSO-Based optimisation algorithm

- 1: **Input:**
 $\hat{P}_{\text{EV},i,t}$ and $\hat{R}_{\text{gen},t}$;
Cost function parameters $(\alpha_1, \alpha_2, c_{\text{loss}}, c_{\text{penalty}})$;
Constraints (Table I).
- 2: **Step 1: Initialization**
- 3: Initialise a population of N particles, where each particle represents a solution: $P_{\text{EV},i,t}, R_{\text{curt},t}$.
- 4: Assign random initial velocities to each particle.
- 5: Define bounds for decision variables:
EV charging power ($0 \leq P_{\text{EV},i,t} \leq P_{\text{EV,max}}$).
Renewable curtailment ($0 \leq R_{\text{curt},t} \leq R_{\text{cap}}$).
- 6: **Step 2: Evaluate objective function**
- 7: **for** each particle in the swarm **do**
- 8: Compute the cost function: $\mathcal{J}_{\text{total}}$ in (1)
- 9: **end for**
- 10: **Step 3: Apply constraints (Table I)**
- 11: **for** each particle **do**
- 12: Check feasibility against the constraints
- 13: **if** particle violates constraints **then**
- 14: Penalise its cost function.
- 15: **end if**
- 16: **end for**
- 17: **Step 4: Update particle position and velocity**
- 18: **for** each particle **do**
- 19: Update velocity and position in (8)
- 20: Ensure particles stay within bounds.
- 21: **end for**
- 22: **Step 5: Termination**
- 23: **if** maximum iterations reached or fitness convergence is achieved **then**
- 24: Terminate the algorithm.
- 25: **else**
- 26: Go to Step 2.
- 27: **end if**
- 28: **Output:**
Optimal EV schedules $(P_{\text{EV},i,t})$.
Optimal renewable curtailment $(R_{\text{curt},t})$.

weather features (temperature, rainfall, humidity), extracted and pre-processed (as detailed in Algorithm 1). Fig. 3 presents a scatter plot of predicted versus actual EV charging demand. The points are tightly clustered around the reference line representing perfect prediction, confirming the accuracy and low variance of the model's output across different demand levels.

B. Renewable generation prediction

Fig. 4 illustrates time-series plots of actual and predicted renewable generation prediction for Bus 02 (with wind farm) and Bus 12 (with PV) using the GB algorithm, discussed in Subsection III-A2. The results demonstrate that the GB model captures the temporal trends and variability of renewable generation effectively (as detailed in Algorithm 2). On Bus 02, where wind is the primary energy source, the model ac-

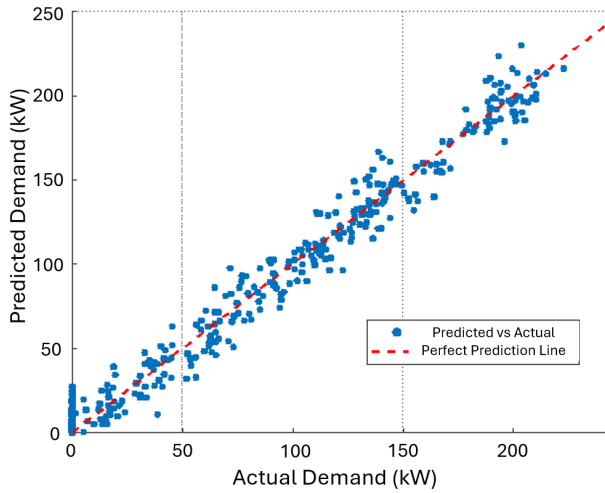


Fig. 3: Simulation results: EV charging demand prediction using RF algorithm.

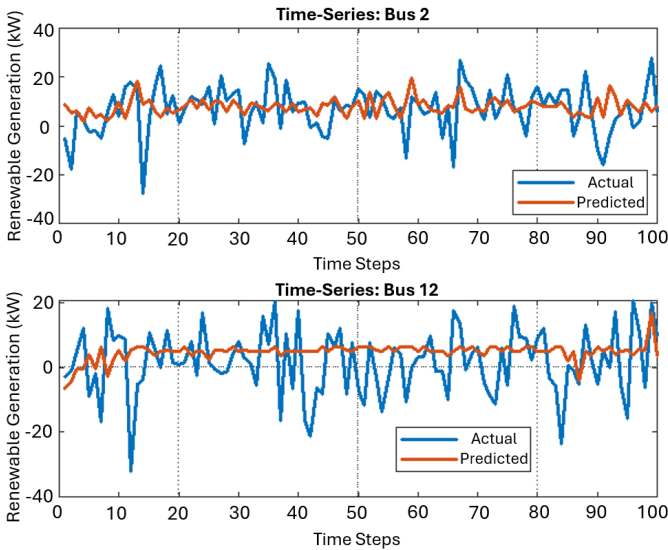


Fig. 4: Time-series comparison between actual and predicted renewable generation using GB algorithm for wind and PV resources, at Bus 02 (top) and Bus 12 (bottom), respectively.

curately follows fluctuations caused by changing wind speeds. Similarly, for Bus 12, where solar irradiance is dominant, the model tracks the diurnal generation pattern with high fidelity. The RMSE value representing the deviations between actual and predicted values is approximately 6.50 kW.

C. Optimisation layer performance

The optimisation layer uses the predicted EV demand $\hat{P}_{EV,i,t}$ and renewable energy generation profiles $\hat{R}_{gen,t}$ obtained from the ML models to solve a multi-objective optimisation problem, as detailed in III-B. The PSO-based algorithm (detailed in Algorithm 3) dynamically adjusts EV charging and renewable curtailment decisions based on the forecasted profiles.

1) *Fairness in EV charging schedules*: Based on the predicted EV demand $\hat{P}_{EV,i,t}$, the optimisation framework ensures balanced charging schedules across all buses. Fig 5 illustrates the distribution of unmet EV demand across different buses before and after optimisation. The box plots show the spread of unmet demand values for each bus, with the blue and red bars representing unmet demand before and after optimisation, respectively. The results demonstrate a significant reduction in unmet demand, as evidenced by the decrease in the median and interquartile range.

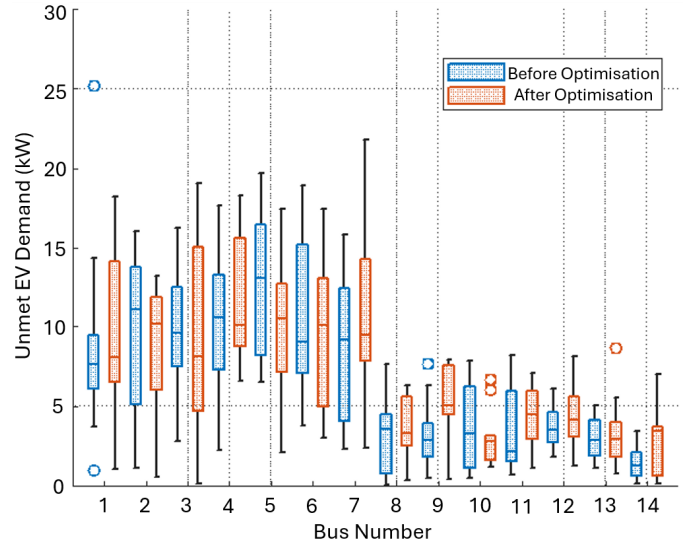


Fig. 5: Unmet EV demand per bus before and after optimisation using PSO algorithm.

2) *Renewable curtailment minimisation*: The optimisation framework prioritised the efficient use of renewable energy based on the predicted RES generation profiles $\hat{R}_{gen,t}$. As shown in Fig. 6, renewable curtailment is reduced from 15% (baseline) to 5%, thus supporting higher renewable integration.

D. Scalability and sensitivity analysis

The scalability of the proposed two-level ML and optimisation framework is assessed by varying the system size in terms of the number of EVs and buses. Three scenarios are tested: a small-scale system (200 EVs and 14 buses), a medium-scale system (400 EVs and 20 buses), and a large-scale system (600 EVs and 30 buses). As summarised in Table II, the prediction accuracy, measured by MAPE, remains within acceptable limits (below 8%) across all system sizes. Although the optimisation time increases with system size, computation times remain within feasible limits for near real-time energy management applications.

TABLE II: Scalability analysis of the proposed framework

System size	Buses	Prediction MAPE (%)	Optimisation time (s)
Small (200 EVs)	14	6.26	12.51
Medium (400 EVs)	20	7.41	28.09
Large (600 EVs)	30	7.87	36.33

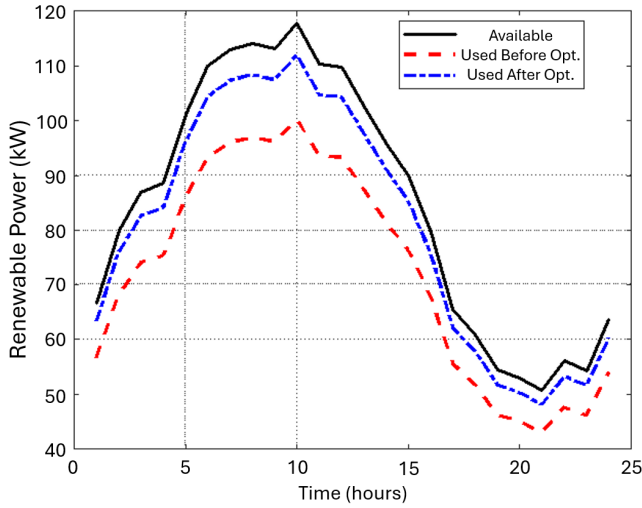
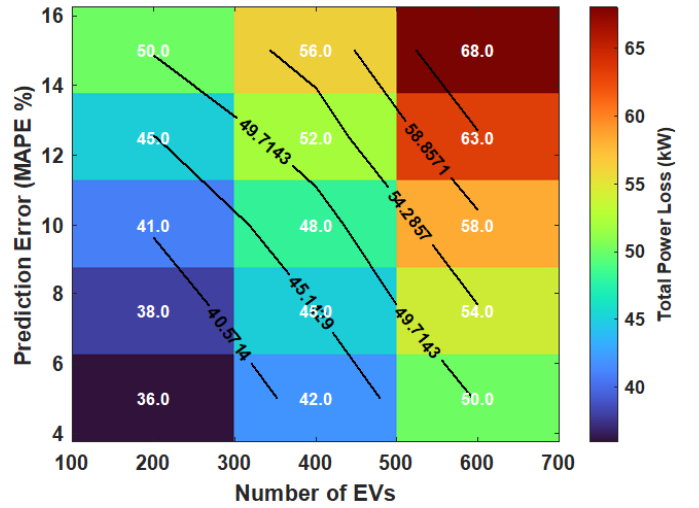


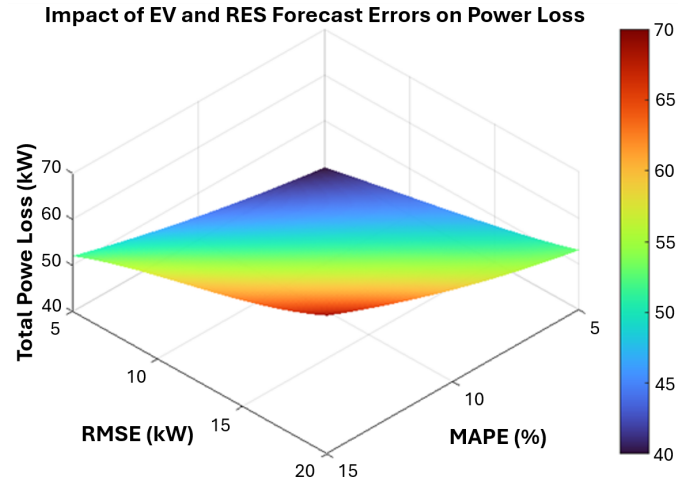
Fig. 6: Renewable energy generation and curtailment profiles before and after optimisation using PSO algorithm.

To evaluate the robustness of the proposed optimisation framework against uncertainties in EV demand and renewable generation forecasts, a sensitivity analysis is performed. Prediction errors are introduced into the forecasted profiles, ranging from 5% to 15% MAPE, to mimic potential inaccuracies from the ML models. Fig. 7a presents a two-dimensional sensitivity map illustrating the impact of varying prediction errors and EV penetration levels on total system power losses. The results reveal a strong correlation between forecast accuracy and optimisation outcomes. Specifically, as MAPE increases, power losses escalate significantly, with the effect becoming more pronounced at higher EV penetrations. For instance, at 500 EVs, increasing MAPE from 5% to 15% leads to a power loss rise of nearly 30%. Contour lines in Fig. 7a highlight regions of equal power losses, emphasising critical thresholds where minor deteriorations in prediction accuracy could cause disproportionate increases in system losses. The influence of renewable generation forecast accuracy is also evaluated using RMSE. The results indicate that as RMSE grows (increasing from 5 kW to 20 kW), total power losses and renewable curtailment rates also rise sharply. For example, beyond 15 kW RMSE, power losses grow by approximately 25–30%. Furthermore, Fig. 7b presents a combined sensitivity surface illustrating the joint effect of EV demand and RES generation forecast errors on total system power losses. The results show that simultaneous high errors in both forecasts lead to non-linear amplification of power losses and curtailment.

To assess the flexibility and robustness of the proposed optimisation framework, a sensitivity analysis is conducted on the cost function weights α_1 and α_2 in eq. (1), which balances the trade-off between minimising power losses and fulfilling EV charging demand. α_1 and α_2 are varied within a range of [0.5, 1, 1.5] around their nominal values (both initially set to 1). Table III summarises the system performance under different weighting scenarios. As expected, increasing α_1 places more



(a) Impact of EV demand prediction accuracy (MAPE)



(b) Combined impact of EV and RES prediction errors (MAPE and RMSE)

Fig. 7: Sensitivity analysis results: Effects of EV and RES forecast errors on system power losses.

emphasis on loss minimisation, resulting in lower power losses but at the cost of higher unmet EV demand. Conversely, increasing α_2 improves EV charging satisfaction but leads to higher power losses due to increased demand fulfilment.

TABLE III: Sensitivity of system performance to cost coefficient variations.

Scenario	α_1	α_2	Power loss	Unmet EV demand
Base case	1.0	1.0	36 kW	12 kW
High loss priority	1.5	1.0	30 kW	18 kW
High EV priority	1.0	1.5	42 kW	5 kW
Equal low priority	0.5	0.5	40 kW	8 kW

E. Comparative analysis

To benchmark the performance of the proposed PSO-based optimisation framework, a comparative analysis is conducted

TABLE IV: Comparative performance analysis of optimisation methods.

Optimisation method	Convergence time (s)	Power loss reduction	Renewable curtailment reduction
PSO	12.51 s	28%	67%
GA	22.12 s	25%	58%
MILP	18.06 s	24%	55%

against two widely used optimisation techniques: GA and MILP. Table IV summarises the key performance indicators for all three approaches, including convergence time, total power loss reduction, and renewable curtailment reduction.

As shown in Table IV, PSO achieves the highest performance in both power loss reduction and renewable curtailment mitigation, significantly outperforming GA and MILP. Specifically, PSO reduces total power losses by 28%, compared to 25% and 24% for GA and MILP, respectively. Moreover, PSO reduces renewable curtailment from 15% (baseline) to 5%, representing a 67% reduction relative to the baseline curtailment, which is substantially higher than the curtailment reductions achieved by GA (58%) and MILP (55%). In terms of computational efficiency, PSO converges within 12.5 seconds, demonstrating its suitability for near real-time energy management applications. By comparison, GA and MILP required longer convergence times of 22.1 s and 18.6 s, respectively.

V. CONCLUSION

This paper presents a two-level ML framework for intelligent energy management in EV- and RES-integrated smart grids. The prediction layer, based on RF and GB, achieves high forecast accuracy, with an MAPE of 6.2% for EV demand prediction and an RMSE of 6.50 kW for renewable generation forecasting. The optimisation layer, using a PSO algorithm, effectively minimises system costs by optimising EV charging schedules and reducing renewable energy curtailment. Case study results demonstrate that renewable curtailment is reduced from 15% to 5%, while fairness in EV charging is significantly improved across the network. The framework maintains robust prediction and optimisation performance as the system scales from small to large grid sizes. Comparative analysis confirms that the PSO approach outperforms GA and MILP in both optimisation effectiveness and computational efficiency. Sensitivity analysis highlights that forecast accuracy is critical for maintaining system reliability, as larger prediction errors substantially increase power losses and curtailment. Future work will explore uncertainty-aware optimisation, online learning, and vehicle-to-grid (V2G) integration to further enhance flexibility and adaptability.

ACKNOWLEDGMENT

The work is supported by the U.K. Leverhulme Trust grant RPG-2023-107.

REFERENCES

- [1] Int. Energy Agency. Global EV Outlook 2024: Moving Towards Increased Affordability. Accessed: March. 14, 2025. [Online]. Available: <https://iea.blob.core.windows.net/assets/a9e3544b-0b12-4e15-b407-65f5c8ce1b5f/GlobalEVO Outlook2024.pdf>.
- [2] F. Nasr Esfahani, A. Darwish, S. Alotaibi and F. Campean, "Hierarchical Control Design of a Modular Integrated OBC for Dual-Motor Electric Vehicle Applications," *IEEE Access*, vol. 12, pp. 196306-196327, 2024.
- [3] F. N. Esfahani, J. Ebrahimi, A. Bakhshai, X. Ma and A. Darwish, "A Modular Bidirectional Topology for Grid-Tied PV Powered EV Chargers with Isolated Single-Stage Sub-Modules," in *IECON 2024 - 50th Annual Conference of the IEEE Industrial Electronics Society*, Chicago, IL, USA, 2024, pp. 1-6.
- [4] L. Xue et al., "A Joint Distributed Optimization Framework for Voltage Control and Emergency Energy Storage Vehicle Scheduling in Community Distribution Networks," *IEEE Transactions on Industry Applications*, vol. 60, no. 4, pp. 5317-5330, July-Aug. 2024.
- [5] R. A. Osama, A. F. Zobaa and A. Y. Abdelaziz, "A Planning Framework for Optimal Partitioning of Distribution Networks Into Microgrids," *IEEE Systems Journal*, vol. 14, no. 1, pp. 916-926, Mar. 2020.
- [6] X. Sun, J. Qiu and J. Zhao, "Real-Time Volt/Var Control in Active Distribution Networks With Data-Driven Partition Method," *IEEE Transactions on Power Systems*, vol. 36, no. 3, pp. 2448-2461, May 2021.
- [7] T. M. Aljohani, A. Saad and O. A. Mohammed, "Two-Stage Optimization Strategy for Solving the VVO Problem Considering High Penetration of Plug-In Electric Vehicles to Unbalanced Distribution Networks," *IEEE Transactions on Industry Applications*, vol. 57, no. 4, pp. 3425-3440, July-Aug. 2021.
- [8] H. Ruan, H. Gao, Y. Liu, L. Wang and J. Liu, "Distributed Voltage Control in Active Distribution Network Considering Renewable Energy: A Novel Network Partitioning Method," *IEEE Transactions on Power Systems*, vol. 35, no. 6, pp. 4220-4231, Nov. 2020.
- [9] L. Tong, S. Zhao, H. Jiang, J. Zhou, and B. Xu, "Multi-scenario and multi-objective collaborative optimization of distribution network considering electric vehicles and mobile energy storage systems," *IEEE Access*, vol. 9, pp. 55690-55697, 2021.
- [10] Y. Zhao, J. Lin, Y. Song, and Y. Xu, "A hierarchical strategy for restorative self-healing of hydrogen-penetrated distribution systems considering energy sharing via mobile resources," *IEEE Trans. Power Syst.*, vol. 38, no. 2, pp. 1388-1404, Mar. 2023.
- [11] Y. Wang, D. Qiu, G. Strbac, and Z. Gao, "Coordinated electric vehicle active and reactive power control for active distribution networks," *IEEE Trans. Ind. Informat.*, vol. 19, no. 2, pp. 1611-1622, Feb. 2023.
- [12] B. Xie, C. Zhu, L. Zhao, and J. Zhang, "A gradient boosting machine-based framework for electricity energy knowledge discovery," *Frontiers in Environmental Science*, vol. 10, p. 1031095, 2022.
- [13] S. M. Putri, M. Ashari, Endroyono and H. Suryoatmojo, "EV Charging Scheduling with Genetic Algorithm as Intermittent PV Mitigation in Centralized Residential Charging Stations," in *2023 International Seminar on Intelligent Technology and Its Applications (ISITIA)*, Surabaya, Indonesia, 2023, pp. 286-291.
- [14] A. Imran et al., "Heuristic-Based Programmable Controller for Efficient Energy Management Under Renewable Energy Sources and Energy Storage System in Smart Grid," *IEEE Access*, vol. 8, pp. 139587-139608, 2020.
- [15] A. D. A. Bin Abu Sofian, H. R. Lim, H. S. H. Munawaroh, Z. Ma, K. W. Chew, and P. L. Show, "Machine learning and the renewable energy revolution: Exploring solar and wind energy solutions for a sustainable future including innovations in energy storage," *Sustainable Development*, vol. 32, no. 4, pp. 3953-3978, 2024.
- [16] N. E. Benti, M. D. Chaka, and A. G. Semie, "Forecasting renewable energy generation with machine learning and deep learning: Current advances and future prospects," *Sustainability*, vol. 15, no. 9, p. 7087, 2023.
- [17] D. Wei and J. Fan, "Optimization strategies for integrating electric vehicle energy storage systems with the new energy Internet: A focus on demand forecasting and grid response," in *Proc. 6th Int. Conf. Commun., Inf. Syst. Comput. Eng. (CISCE)*, Guangzhou, China, 2024, pp. 148-152.